ISBN: 978-3-95450-262-2 ISSN: 2673-5350 doi: 10.18429/JACoW-IBIC2025-MOPCO34

DEVELOPMENT OF BPM ELECTRONICS FOR KOREA 4TH GENERATION STORAGE RING

Siwon Jang*, Dongcheol Shin, Pohang Accelerator Laboratory, Pohang, South Korea

Abstract

New BPM electronics have been developed for installation in the storage ring of the 4th Generation Synchrotron Radiation Facility (4GSR) in Ochang, Korea. Based on the first prototype, two different platforms were implemented for the second prototype: an RFSoC-based system optimized for high-performance and broadband data acquisition, and a uTCA-based system designed for long-term maintainability. This paper describes the design, hardware implementation, and test results of both prototypes, including resolution, stability, and compensation methods using crossbar switching. Beam test results at PLS-II are presented and compared with the requirements for the Korea-4GSR storage ring.

INTRODUCTION

The Korea 4th Generation Storage Ring (4GSR) [1], under construction in Ochang, is designed as a diffraction-limited facility with a target emittance nearly 100 times smaller than the existing third-generation PLS-II. This drastic reduction enables ultra-high brilliance photon beams for advanced research in materials science, biology, and industry. Achieving nanometre-level orbit stability under such conditions requires the development of high-performance beam position monitor (BPM) electronics.

The BPM electronics must deliver high-resolution beam position data at multiple acquisition rates—Turn-by-Turn (TbT), Fast Acquisition (FA), and Slow Acquisition (SA)—for orbit feedback, interlock, and closed-orbit determination. To meet long-term stability requirements, two complementary platforms are being developed: an RFSoC-based system for broadband acquisition and future bunch-by-bunch (BbB) capability [2, 3], and a uTCA-based system optimized for integration and maintainability. The design specifications of the BPM electronics are summarised in Table 1.

KOREA 4GSR BPM ELECTRONICS

The system architecture is shown in Fig. 1. Pickup signals are digitised and processed in the BPM electronics, with machine clock and trigger distributed via the event system. Beam position data are transmitted over SFP/SFP+ links to the FOFB, interlock, event system, and fast DAQ, ensuring support for both fast and slow control loops.

The internal data flow is illustrated in Fig. 2. Buffered ADC data are separated into TbT, FA, and SA streams: TbT supports feedback and interlock, FA feeds the fast DAQ, and SA is decimated to 10 Hz for EPICS-based closed-orbit determination.

* siwon@postech.ac.kr

Table 1: Design Specifications of 4GSR BPM Electronics

Quantity	Requirement
TbT position	375 kHz, ≤1 μm
FA position	15.6 kHz, ≤200 nm
SA position	10 Hz, ≤20 nm
Long-term stability	≤±0.2 μm within ±0.5 °C
Data streaming	SFP to FOFB/FOI/Fast DAQ
Future option	BbB monitoring (RFSoC version)

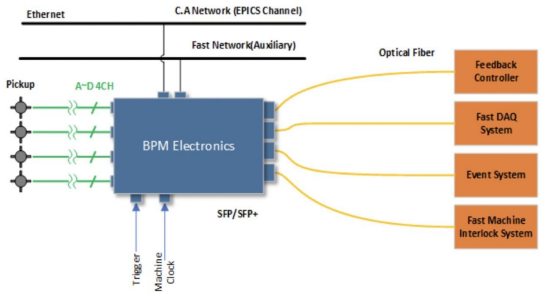

Figure 1: System overview of the BPM electronics.

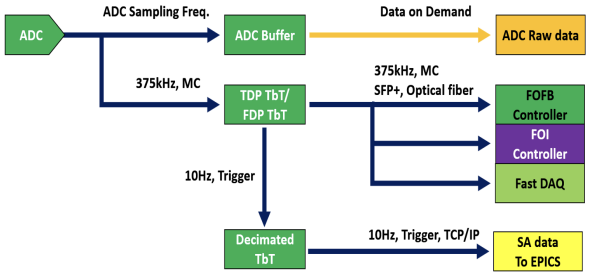

Figure 2: Data flow inside the BPM electronics. ADC raw data are processed into TbT, FA, and SA streams.

RFSoC BPM Electronics

The RFSoC BPM electronics employ interchangeable AFEs (500 MHz narrowband and 2 GHz wideband) with a 2.5 GS/s ADC and FPGA-based processing. A key feature is the integrated crossbar, which removes offset errors from gain and phase mismatches, thereby ensuring the SA 20 nm specification and enhancing long-term stability.

The prototype (Fig. 3) integrates all required I/O, including SMA inputs, SFP+ streaming, Ethernet, and timing interfaces on the front panel. The rear panel provides AC power with EMI filtering, cooling fans, debug, and auxiliary network access. This prototype has passed factory acceptance tests (FAT) and will be evaluated with beam at PLS-II prior to 4GSR installation [3, 4].

Performance of RFSoC BPM Electronics

The performance of the RFSoC BPM electronics was evaluated through measurement and simulation. Figure 4

ISBN: 978-3-95450-262-2 ISSN: 2673-5350 doi: 10.18429/JACoW-IBIC2025-MOPCO34

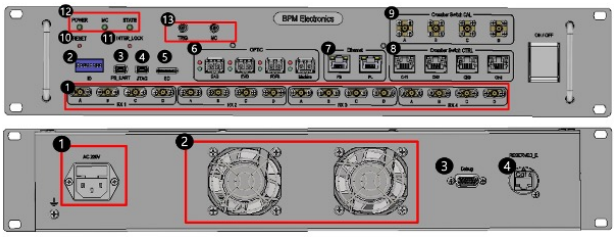

Figure 3: Prototype RFSoC BPM electronics: front and rear panel layout. Port numbers correspond to descriptions in the text.

shows RMS noise versus input power, where CW signals from 0 to −62 dBm were injected and both TbT and FA data acquired. RMS noise decreases with increasing input power, following a $1/\sqrt{N}$ trend, with FA achieving about five times better resolution than TbT. For −26 to 0 dBm, AFE gain was adjusted to fully utilize the ADC range. These results confirm sub-micron TbT and 200 nm FA resolution requirements for 4GSR.

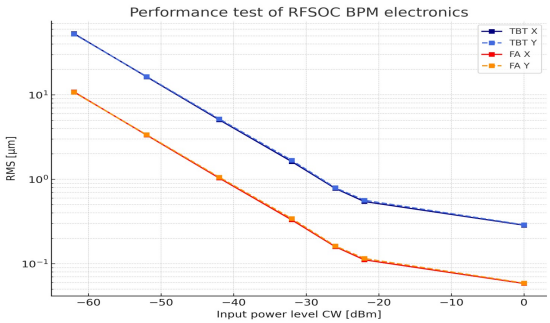

Figure 4: Measured RMS noise dependence on input power level. FA performance shows consistently better resolution than TbT, meeting the Korea 4GSR required specifications.

Figure 5 presents the simulation setup used to study the impact of channel-to-channel gain differences combined with temperature drifts and AC power coupling. The four panels reproduce trends consistent with experimental observations, confirming that gain mismatch and thermal effects jointly influence the stability of SA data. The lower-right panel further highlights the effectiveness of crossbar switching, which compensates offset errors and significantly improves the long-term stability of beam position measurements.

The observed SA drift can be modeled as the combined effect of channel gain mismatches, temperature-dependent variations, and AC ripple coupling. For a given pickup channel i, the effective gain can be expressed as

$$G_i(t) = G_{i0} + \Delta G_i(T(t)) + \Delta G_i^{\mathrm{AC}}(t), \tag{1}$$

where G_{i0} is the nominal gain, $\Delta G_i(T(t))$ represents the temperature-dependent variation, and $\Delta G_i^{\mathrm{AC}}(t)$ denotes the AC ripple component (e.g. 60/120 Hz).

The measured beam position $X_{\mathrm{meas}}(t)$ is then given by

$$X_{\mathrm{meas}}(t) = \frac{\sum_{i=1}^{4} G_i(t) S_i(t)}{\sum_{i=1}^{4} G_i(t)}, \tag{2}$$

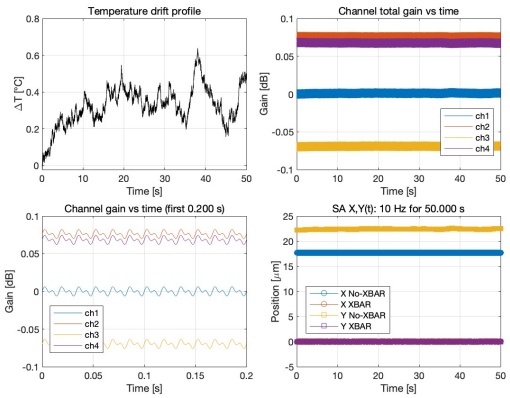

Figure 5: Simulation framework for temperature drift and AC-coupled gain ripple. Top-left: $\Delta T(t)$ profile; top-right: total gain evolution across four channels; bottom-left: zoomed channel gain ripple; bottom-right: SA positions at 10 Hz with and without crossbar.

where $S_i(t)$ is the signal from pickup i. Without correction, the time-dependent gain terms introduce offsets that accumulate in the SA averaging process.

When the crossbar switch is applied, each pickup signal is cyclically routed through all AFE channels, such that the effective gain becomes

$$\bar{G}(t) = \frac{1}{N} \sum_{j=1}^{N} G_j(t), \tag{3}$$

where N is the number of switching states. This averaging cancels first-order gain mismatches and suppresses temperature-dependent drifts.

Figure 6 compares simulated $\sigma(N)$ curves (No-XBAR and XBAR) with those reconstructed from TbT data. Without the crossbar, the standard deviation deviates from the $1/\sqrt{N}$ law beyond a few hundred turns, saturating near 60 nm due to gain mismatch and drift. With crossbar, the scaling follows the ideal trend, from ~800 nm at $N = 1$ to ~4–5 nm at $N =$ 37500. Measurements show slightly higher values (5–7 nm), while direct SA data yield 10–20 nm even with crossbar. These results confirm the crossbar is essential to meet the 4GSR stability goal.

uTCA BPM Electronics

The uTCA-based BPM electronics are being developed as a platform-oriented solution to ensure long-term maintainability and system scalability. The design adopts newly developed RTM (Rear Transition Module) boards in combination with commercially available AMC (Advanced Mezzanine Card) modules, thereby reducing development effort while maximizing flexibility for future upgrades.

Initial prototype measurements have already demonstrated sub-micron performance, achieving better than 1 µm resolution in TbT data. Ongoing work is focused on optimizing additional functionalities, including FA and SA data paths, timing interfaces, and integration with accelerator control systems. Figure 7 shows the fabricated prototype, including front-side and back-side views.

ISBN: 978-3-95450-262-2 ISSN: 2673-5350 doi: 10.18429/JACoW-IBIC2025-MOPCO34

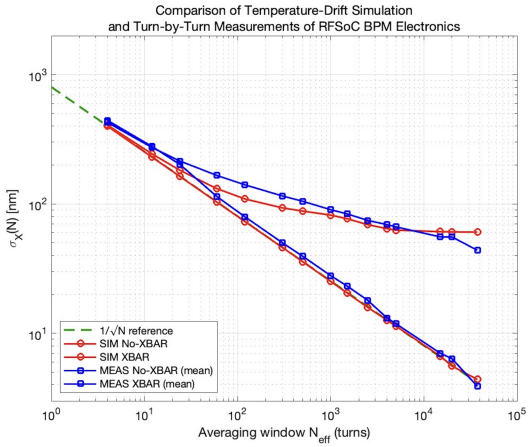

Figure 6: Simulation and measurement of $\sigma(N)$. Crossbar restores near-ideal $1/\sqrt{N}$ scaling to few-nm resolution, while No-XBAR saturates at tens of nanometres.

The most significant advantage of the uTCA approach lies in its platform-based design philosophy, which facilitates modular replacement, simplifies maintenance, and enables mass production with standardized components. This ensures that the system can be efficiently supported throughout the lifetime of the 4GSR project.

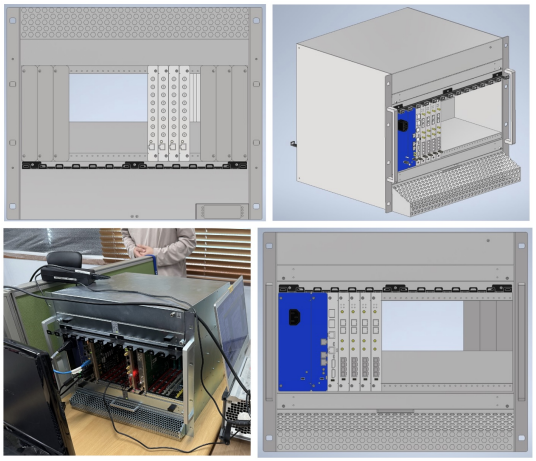

Figure 7: Prototype uTCA BPM electronics with newly developed RTM boards and commercial AMC modules. Front-side and back-side views are shown.

Crossbar Switch Implementations

Two types of crossbar switches have been developed to support the 4GSR BPM electronics, each optimized for different system requirements.

The first design, used in the RFSoC BPM electronics, adopts a simplified structure where each BPM pickup signal is routed through only two switching stages before reaching the AFE inputs. This approach minimizes insertion loss and simplifies implementation, but the achievable isolation is limited to about 50 dB, as illustrated in Fig. 8 (top).

The second design, developed for the uTCA BPM electronics, integrates a 4 × 4 switching matrix. In this scheme, signals pass through multiple switch elements before reaching the outputs, increasing routing flexibility and providing higher isolation (approximately 65 dB). Figure 8 (bottom) shows the layout of the 4 × 4 crossbar design and a fabricated PCB prototype. Although the architecture introduces greater complexity and footprint, it offers improved suppression of channel coupling and long-term stability, which is particularly beneficial for SA measurements where thermal drifts and gain mismatches accumulate.

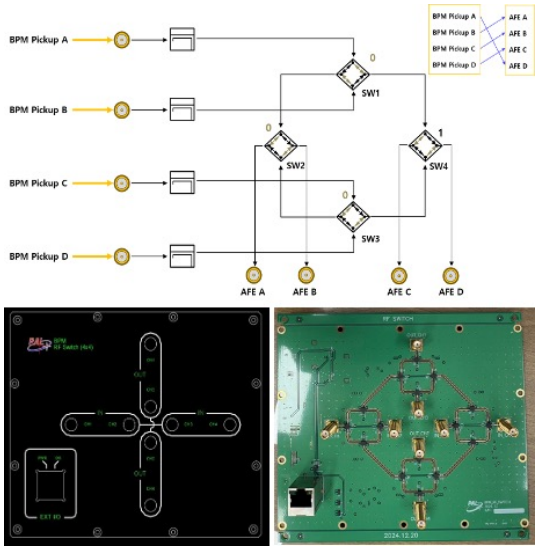

Figure 8: Two types of crossbar switch: (top) simplified RFSoC version with two-stage routing; (bottom) layout of the 4 × 4 crossbar design and fabricated PCB prototype of the uTCA version.

CONCLUSIONS

The Korea-4GSR BPM electronics were developed to meet the stringent stability requirements of a diffraction-limited light source using two platforms: an RFSoC-based system for broadband acquisition and future bunch-by-bunch monitoring, and a uTCA-based system for modularity and maintainability.

Prototype tests of the RFSoC version achieved sub-micron TbT and nanometer-level FA/SA performance, with crossbar switching reducing SA noise from 50–70 nm to 10–20 nm. The uTCA version demonstrated<1 µm TbT resolution and offers clear serviceability advantages. Two crossbar switch designs were implemented, balancing simplicity and higher isolation. Both platforms will be validated at PLS-II prior to 4GSR deployment, ensuring readiness for nanometer-level orbit stability.

ACKNOWLEDGMENTS

This research was supported in part by the Korean Government(MSIT: Ministry of Science and ICT) (No. RS-2022-00155836, Multipurpose Synchrotron Radiation Construction Project) and also supported by Pohang Accelerator Laboratory (PAL). PAL is supported by Korean Government(MSIT) and POSTECH.

ISBN: 978-3-95450-262-2 ISSN: 2673-5350 doi: 10.18429/JACoW-IBIC2025-MOPCO34

REFERENCES

[1] G. S. Jang *et al.*, "Low emittance lattice design for Korea-4GSR", *Nucl. Instrum. Methods Phys. Res. A*, vol. 1034, p. 166779, 2022. doi:10.1016/j.nima.2022.166779

[2] S.-W. Jang, "Development of Button BPM Electronics for the BbB Feedback System of 4GSR", in *Proc. IPAC'22*, Bangkok, Thailand, Jun. 2022, pp. 332–334. doi:10.18429/JACoW-IPAC2022-MOPOPT038

[3] S.-W. Jang *et al.*, "Developments of 4GSR BPM Electronics", in *Proc. IBIC'23*, Saskatoon, Canada, Sep. 2023, pp. 87–89. doi:10.18429/JACoW-IBIC2023-MOP030

[4] S.-W. Jang, D. Shin, S. Ahn, D. Kim, and B. Shin, "Development of High-Precision Beam Position Monitor for the Korean 4GSR Project", in *Proc. IBIC'24*, Beijing, Sep. China, 2024, pp. 118–121. doi:10.18429/JACoW-IBIC2024-TUP30